Lasers in Manufacturing Conference 2019

Holistic sensor concept for process control and quality assurance in laser beam welding based on Optical Coherence Tomography

Christian Stadter[a*], Maximilian Schmoeller[a], Markus Kogel-Hollacher[b], Ulrich Munzert[c], Michael F. Zaeh[a]

[a]*Institute for Machine Tools and Industrial Management, Technical University of Munich, Boltzmannstr. 15, 85748 Garching, Germany*
[b]*Precitec GmbH & Co. KG, Draisstr. 1, 76571 Gaggenau, Germany*
[c]*Blackbird Robotersysteme GmbH, Carl-Zeiss-Str. 5, 85748 Garching, Germany*

Abstract

Optical Coherence Tomography (OCT) enables the acquisition of direct information about the geometry of the process zone during laser beam welding. The measuring principle allows for spatial and temporal highly accurate measurements that are hardly affected by process emissions or metal vapor/plasma. A novel sensor concept based on OCT was evaluated for both multi-mode and single-mode laser radiation as well as for fixed and remote optics. The sensor was attached to a 3D scanner unit allowing for measurements before, in, and after the process zone. Fundamental studies on aluminum, copper, and galvanized steel were carried out to analyze the effect of the material, the process, and the measurement parameters. Scan lines before and after the process zone were applied for tracking edges and assessing the weld seam topography during the process in real-time. Measurements coaxial to the laser beam revealed the capillary depth for spot sizes down to 55 µm.

Keywords: Optical Coherence Tomography; In Situ Weld Depth Measurement; Process Control; Quality Assurance; Laser Beam Welding

1. Introduction

Optical Coherence Tomography (OCT) has unique capabilities regarding a direct process observation during laser beam welding. Current studies aim at systems that allow a direct quality assurance or process control on the basis of in situ process data. Despite the high demands on the observation methods resulting from the high process dynamics and the intense process emissions, OCT enables a direct measurement of the topology within the process zone. In contrast to conventional methods, which are either based on the evaluation of indirect quantities, such as secondary emissions, or costly offline tests, the geometrical

information recorded by OCT allow for a robust interpretation independent of disturbances such as metal vapor and plasma generated during welding.

In order to use the spatially and temporally high-resolution measurement data for inline quality evaluation and process control purposes, a fundamental understanding of the highly dynamic effects of the welding process on the sensor data is necessary. A precise knowledge of the effects and disturbances affecting the measurement is the basis to fully exploit the potential of this technology for the use in all areas relevant for laser beam welding.

2. Optical Coherence Tomography

The functional principle of OCT is based on the interferometer design proposed by A. A. Michelson, cp. Fig. 1 (a). A broadband light source rather than a narrow-band laser beam source is used to generate the measuring beam. OCT as a procedure is therefore often referred to as Low Coherence Interferometry and also known as White Light Interferometry. The technique has been utilized since 1972 to perform high-precision distance measurements (FLOURNOY ET AL. 1972). OCT has been used primarily to capture topographic images of the eye since a lateral scanning device could be integrated into the beam path in 1991 (HUANG ET AL. 1991). Demonstrating that a fraction of 10^{-10} of the incident optical power reflected at the measuring object is sufficient to perform a distance measurement, the work of HUANG ET AL. (1991) supported the subsequent establishment of OCT in ophthalmology. Further development enabled the evaluation of the interference in the frequency domain (FD) rather than in the time domain (TD) (CHINN ET AL. 1997), allowing for drastically reduced acquisition times for topographic scans with higher sensitivities than in the TD (BOER ET AL. 2003). This made high-precision distance measurements (FRASER 2012) at scan rates of several kilohertz possible. (BERNARDES AND CUNHA-VAZ 2012)

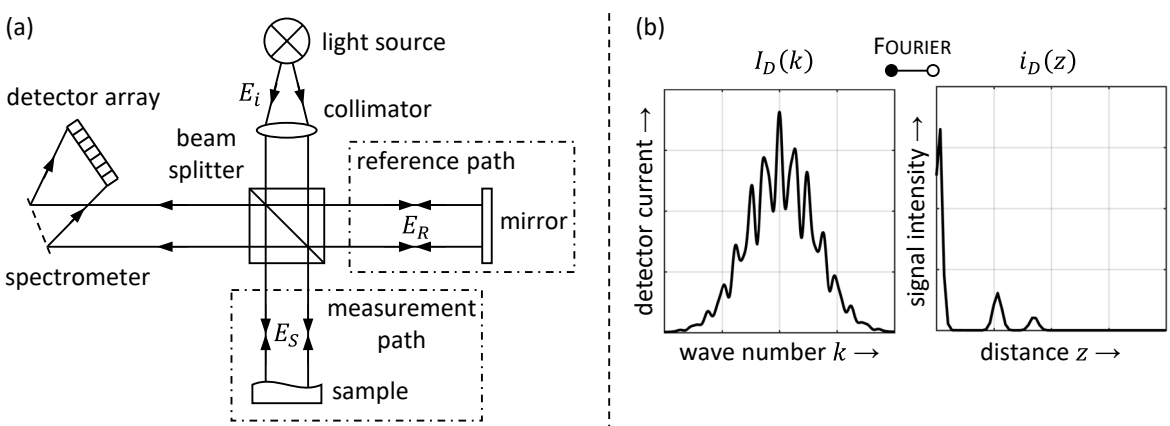

Fig. 1. (a) optical concept of Fourier Domain OCT; (b) raw detector signal as a function of the wave number and Fourier transformed signal in FD OCT (based on DONGES AND NOLL (2015))

With the polychromatic illumination with the electric field in complex form

$$E_i = s(k,\omega)e^{i(kz-\omega t)}, \qquad (1)$$

and the assumption of a constant and wavelength independent splitting ratio of 0.5 of the beam splitter, the electric fields in the reference and measurement path (cp. Fig. 1 (a)) can be determined according to DREXLER (2008):

$$E_R = \frac{E_i}{\sqrt{2}} r_R e^{i2kz_R},\ E_S = \frac{E_i}{\sqrt{2}} \sum_{n=1}^{N} r_{Sn} e^{i2kz_{Sn}} \tag{2}$$

Here, s is the amplitude of the electric field as a function of the wave number k and the angular frequency ω, z the coordinate in beam propagation direction, and t the time. Multiple reflections n at the positions z_{Sn} with the respective power reflectivity $R_{Sn} = |r_{Sn}|^2$ are considered for the general case of transparent media. The photocurrent I_D in the detector results from the superposition of the electric fields from the reference and the measurement path (DREXLER 2008):

$$I_D(k,\omega) = \frac{\rho}{2} \langle |E_R + E_S|^2 \rangle \tag{3}$$

ρ describes the responsivity of the sensor and $\langle \cdot \rangle$ is the time average, i.e. the integration over the response time of the detector $\langle f \rangle = \lim_{T\to\infty} \frac{1}{2T} \int_{-T}^{T} f(t)dt$ (BERNARDES AND CUNHA-VAZ 2012). With equations 1 and 2, the temporally invariant terms of the detector current can be calculated as follows (DREXLER 2008):

$$\begin{aligned} I_D(k) &= \frac{\rho}{4}[S(k)(R_R + R_{S1} + R_{S2} + \dots)] \\ &+ \frac{\rho}{4}\left[S(k) \sum_{n=1}^{N} \sqrt{R_R R_{Sn}} \left(e^{i2k(z_R - z_{Sn})} + e^{-i2k(z_R - z_{Sn})}\right)\right] \\ &+ \frac{\rho}{4}\left[S(k) \sum_{n\neq m=1}^{N} \sqrt{R_{Sn} R_{Sm}} \left(e^{i2k(z_{Sn} - z_{Sm})} + e^{-i2k(z_{Sn} - z_{Sm})}\right)\right] \end{aligned} \tag{4}$$

The spectral power as a function of the wave number $S(k)$ can be further simplified. Assuming that the spectral characteristics of light sources typically used for FD OCT correspond to a Gaussian shaped spectrum, the spectral power becomes (DREXLER 2008):

$$S(k) = \langle |s(k,\omega)|^2 \rangle = \frac{1}{\Delta k \sqrt{\pi}} e^{-\left[\frac{k-k_0}{\Delta k}\right]^2} \tag{5}$$

Here, k is the central wave number and Δk the spectral bandwidth of the light source spectrum. To obtain the distance z_S, the expression $\sqrt{R_S(z_S)}$ can be quoted for the case of discrete reflections N as the sum $\sum_{n=1}^{N} \sqrt{R_{Sn}} \delta(z_S - z_{Sn})$. The result of the inverse Fourier transformation of equation 4 can be seen exemplarily in Fig. 1 (b).

3. State of the art

For monitoring laser processes in general and laser beam welding in particular, optical methods are typically used due to their non-contact principle and the high accuracy (LEE AND NA 2002). In the following,

the preliminary studies will be discussed starting with the pre-process zone, continuing with the process zone up to the post-process zone. Regarding the pre-process zone, two systems have been established: laser triangulation and direct observation, typically by means of grayscale images, are applied for seam detection purposes (LUO ET AL. 2012).

MATSUI AND GOKTUG (2002) presented a robot-based arc welding system for seam tracking in thin plate welding utilizing laser triangulation. The height information acquired by orthogonal scans in the advance of the process zone could be used to determine the weld trajectory along edges and to adjust the position of the robot tool. Welding speeds of up to 2 m/min could be achieved using a scan rate of 60 Hz.

LEE ET AL. (2000) developed a system based on optical triangulation to join washer-shaped discs. A geometrical model and different angles of incidence were used to account for the different welding situations for inner and outer edge welding. The geometrical model was extended by image-processing procedures and algorithms capable of tracking the weld seam trajectory. The positioning by means of a two-axis Cartesian stage allowed for tolerances in the positioning of the laser beam of smaller than 50 µm for a welding speed of 22 mm/s.

LUO ET AL. (2012) utilized laser triangulation combined with a coaxial process observation by a camera. The camera was used to cover a pre-running range of 30 mm and thus to enhance the robustness of the tracking algorithm. Different control algorithms were discussed with the intention to process the data as effectively as possible. Tracking errors of ± 0.1 mm on average could be achieved. DORSCH ET AL. (2015) also used both, optical observation by a process camera and laser line projectors. The sensor system was mounted to a scanning optics system, demonstrating the applicability of this approach to remote laser beam welding.

BLECHER ET AL. (2014) performed capillary depth measurements by laser interferometry. They compared the optical sensor data with metallographic sections for various metal alloys. The good correspondence between sensor data and cross sections indicates the applicability of the measurement method for real-time keyhole depth measurements. Thus, also the formation of the keyhole growth during the initiation of deep welding could be observed and compared to theoretically calculated growth rates.

KOGEL-HOLLACHER ET AL. (2016) developed a system for in-situ measurements of the keyhole depth in laser processing based on short coherence interferometry. Studies on the measurement accuracy assessed the effect of the focus diameter of the laser beam, the welding speed, the material and the position of the measuring spot relative to the processing laser on the measurement result. An accuracy of less than ± 10 µm could be achieved for typical process regimes.

FETZER ET AL. (2017) compared high-speed X-ray images with inline capillary depth measurements recorded by OCT. The X-ray images could be used to extract the capillary depth and to calibrate a noise reduction filter for the OCT measurements. The acquisition rate of the OCT system was 70 kHz and that of the X-ray system approx. 1 kHz. Based on the OCT measurements, the influence of a sinusoidal modulation with varying frequencies of the laser power on the capillary depth could be evaluated.

RODRÍGUEZ-GONZÁLVEZ ET AL. (2017) used laser scanning and macro photogrammetry to assess the topography of weld seam surfaces. The measurements were applied after the joining process and allowed the quality of welds to be evaluated in tungsten inert gas welding. The methods developed for the 3D reconstruction were capable of resolving the weld seam surfaces with submillimeter precision.

KOGEL-HOLLACHER ET AL. (2017) discussed ultrafast as well as inline measurements for micro and macro laser processing. A chromatic line sensor was applied to measure the topography of surfaces. The measuring principle allowed for measurements to be taken even on polished, sloped surfaces with up to 400,000 points per second at submicron resolution. OCT was employed for in situ measurements during laser processing. Scans at 70 kHz could be taken from the surface independent of the surface processing by means of ultrashort laser pulses.

WEBSTER ET AL. (2014) applied OCT to monitor the machining depth in remote processing. The measurements could be exploited to develop an automatic sculpting process of 3D structures. The approach was then further enhanced to enable a closed-loop feedback control for an automated laser processing. The machining depth measured at 230 kHz could be evaluated with an axial resolution of about 7 µm (JI ET AL. 2015).

4. Objectives and approach

The great potential of Optical Coherence Tomography by a direct in situ process observation for laser-based machining processes can make a significant contribution to the applicability of laser beam welding for a broad range of industries. For this, however, a precise knowledge of the influencing factors on the sensor system is required. Therefore, fundamental investigations of the influencing factors were performed to qualify the measurement method for a robust use in all zones relevant for laser beam welding. Inline as well as offline tests were performed to assess the effect of process emissions on the accuracy and validity and to evaluate the applicability of OCT for edge tracking, welding depth and topographic measurements.

5. Experimental setup

The tests were carried out using a system based on FD OCT for coaxial distance measurements. Fig. 2 shows the integration of the sensor system into the remote welding system as well as the working space of the remote scanner system.

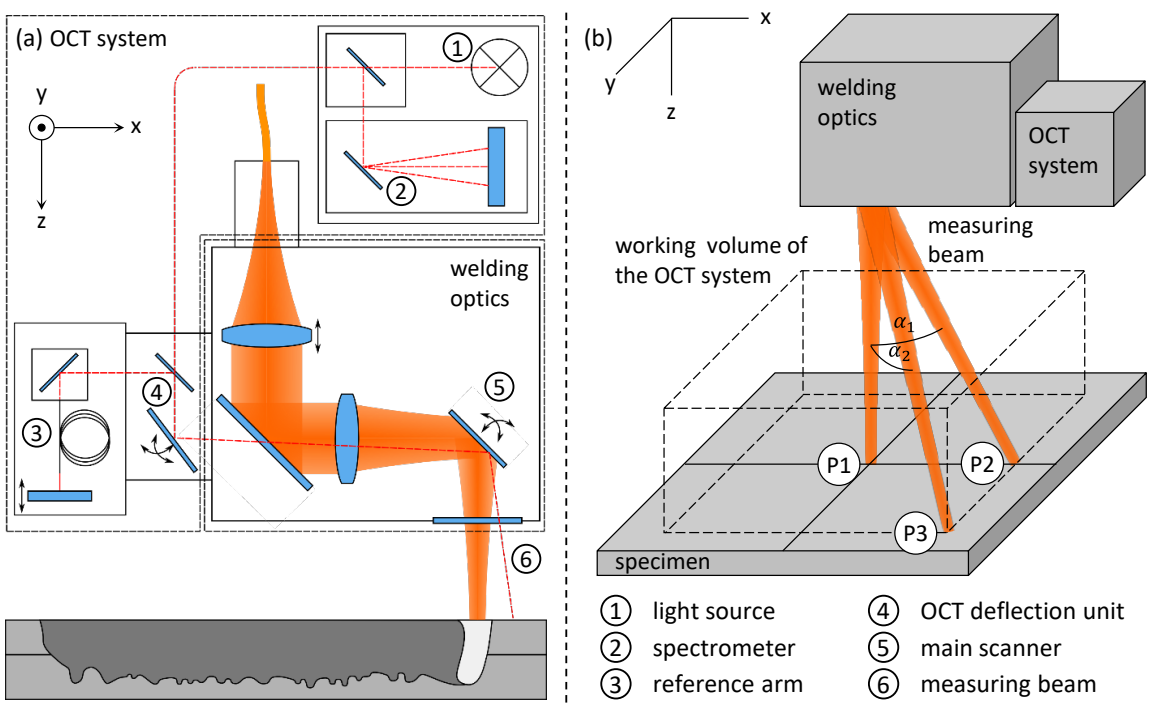

Fig. 2. (a) optical setup of the welding optics equipped with the FD OCT sensor system; (b) characteristic points within the working volume of the scanning optics (based on STADTER ET AL. (2019))

The sensor of the type Precitec IDM provided an acquisition rate of 70 kHz. The spot size of the measuring beam was about 50 µm in the focal plane. The measuring beam passed through the same optical path as the processing beam and could be deflected separately by an independent auxiliary scanner. The analyses of the welding depth were performed with a fixed optics system using multimode and singlemode laser radiation. Details on the respective optical parameters can be found in SCHMOELLER ET AL. (2019) and STADTER ET AL. (2019). With a view to automotive applications, the medium-strength, curable aluminum alloy AA6082 (thickness 4 mm), the galvanized steel HCT780X+Z100 MB (0.75 mm) and the oxygen-free copper alloy C10200 (3 mm) were used in the experiments. The measurements were validated by a Keyence VR 3100 3D macroscope, equipped with a micro and a macro camera.

6. Results

Starting with fundamental investigations on the signal characteristics, the effects of fundamental influencing factors on the measurement are discussed. This allows the OCT measurements to be systematically investigated in all areas relevant to laser beam welding.

6.1. Fundamental signal characteristics

With view to the quality of the distance measurements, the inverse Fourier transformed signal provides information about the signal quality. Fig. 3 shows the spectra in the frequency domain depending on the material and the distance of the measurement beam to the focal plane. Based on a Gaussian fit, the signal-to-noise ratio (SNR) as the ratio of the peak height and the background noise can be used as a measure of the signal quality.

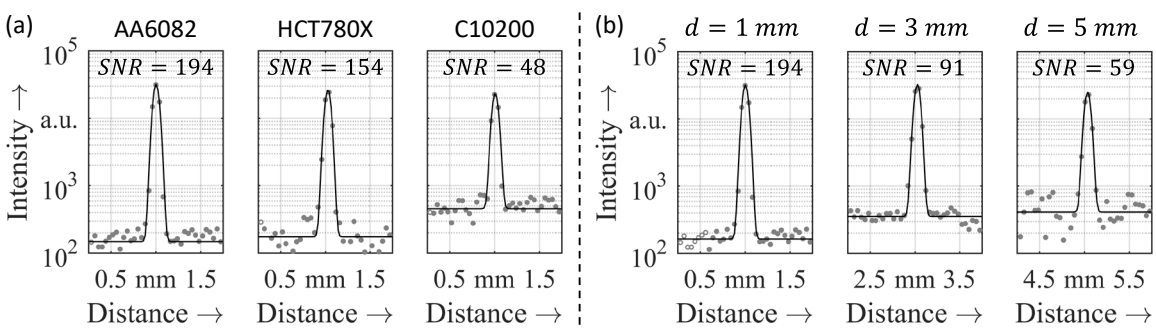

Fig. 3. (a) Fourier transformed spectra depending on the material (a) and the distance to the focal plane (b) (measuring position P1, based on STADTER ET AL. (2019))

The best signal quality can be achieved with aluminum. A decrease in peak height and an increase in background noise result in a slight drop in the SNR for steel. Measurements on copper showed a significantly reduced signal quality of about a quarter of that of aluminum. Regarding the distance to the focal plane d, a steep drop in the SNR could be seen with increasing distance, mainly caused by a rise in background noise. The resulting drop in SNR lies in the exponential falloff in sensitivity (DREXLER 2008) due to a finite spectral resolution of the spectrometer and sampling effects in the Fourier transformation (DREXLER AND FUJIMOTO 2015). A more detailed discussion of the influencing factors can be found in STADTER ET AL. (2019).

6.2. Pre-process zone – edge tracking

The capability of the sensor system for tracking purposes was evaluated exemplarily for fillet welds with varying plate thicknesses, welding speeds and materials. An essential factor for the reliability of the tracking system is the quality of the surface recordings. The robustness of the OCT-based approach can be seen in the SNR of topographic scans shown in Fig. 4 (a). Systematic effects could be observed with the increase in the angle of incidence from position P1 to P3 and the varying distance to the focal plane from the top (t) and bottom (b) plate. For all configurations, the SNR was far above the critical value of about 30, below which the measurement is considered invalid as the distance can no longer be clearly identified. The lowest SNR could be observed on the top plate of the aluminum samples at maximum scanner deflection, but with an average of about 100 it was far above the critical threshold of 30.

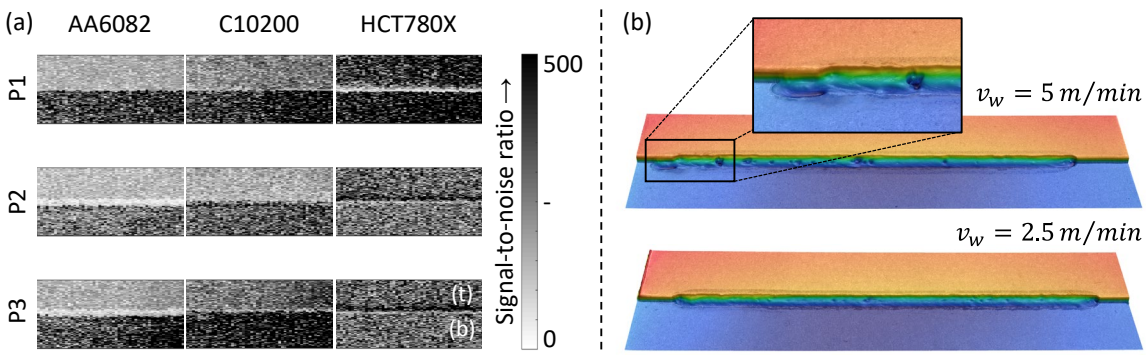

Fig. 4. (a) SNR depending on the position and the material; (b) validation of the real-time seam tracking (HCT 780X, P2, $P_L = 1.4 - 2.4\ kW$, line distance 700 µm, point distance 50 µm; based on STADTER ET AL. (2019))

The accuracy and the robustness with regard to process emissions during welding were evaluated by inline tracking trials on galvanized steel in measurement position 2 (cp. Fig. 2 (b)). The sample topography was recorded by subsequent measurements using a 3D macroscope, see Fig. 4 (b). Two welding speeds were analyzed. Absolutely no deviation from the nominal trajectory could be detected for a welding speed of 2.5 m/min. Increasing the welding speed to 5 m/min did not affect the accuracy of the tracking approach, only the detailed section at the weld seam start showed a lateral deviation. This originated from the measurement time for the initial search of the edge position before the laser had been switched on, which in this case was not sufficient to align the laser spot on the edge in time. Apart from that, the laser spot then precisely followed the target trajectory.

6.3. Process zone – capillary depth measurement

In situ measurements of the welding depth in bead on plate welds were performed using a fixed optics system equipped with a sensor of the type Precitec IDM. A beam splitter allowed to deflect a fraction of the measuring radiation coaxial to the laser beam with a lateral deviation of approx. 5 mm. This facilitated the measurement not only of the capillary depth but also of the distance between the optics and the surface of the material to be welded. Tolerances of the robot-based positioning of the optics could be compensated by calculating the difference between the distance values of the surface and the keyhole.

Fig. 5 (a) illustrates the influence of the welding depth on the signal characteristics. A significant loss in signal density that can be obtained from the capillary can be observed with increasing welding depths. The fluctuations in the measured welding depth indicate an increase of the melt pool dynamics. For large welding depths, the measured depth does not follow the real welding depth exactly, indicating that melt pool dynamics significantly contribute to the formation of the weld seam geometry.

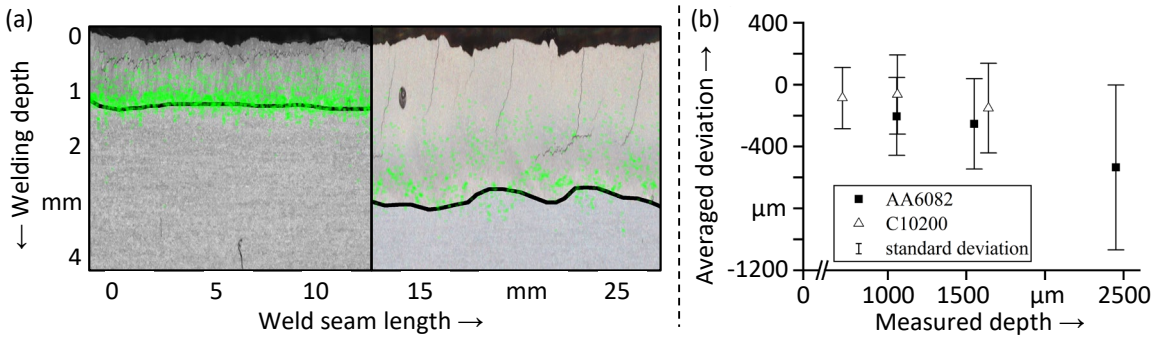

Fig. 5. (a) influence of the welding depth on the signal characteristics; (b) averaged deviation between measured and real welding depth as a function of the measured depth (AA6082; based on SCHMOELLER ET AL. (2019))

Metallographic longitudinal sections were taken to validate the OCT measurements and to assess the deviation to the real welding depth. The deviation averaged over 3 individual tests is shown in Fig. 5 (b). A good correlation for medium depths could be found, whereas the deviation increased for higher welding depths. Also, the uncertainty of the measurement increased as the standard deviation rose with the welding depth. The standard deviation and the decreasing signal density at large welding depths result from the high process dynamics and underline the need for suitable evaluation strategies to interpret the sensor data validly. A statistical discussion of the influence of the material, the angle of incidence of the processing laser beam, the weld depth and the beam characteristics on the sensor data is given by SCHMOELLER ET AL. (2019).

6.4. Post-process zone – quality assurance

Topographic scans in the post-process zone were carried out to assess the quality of the weld seam surface. The measurements were applied inline and offline to evaluate the accuracy of the measuring system considering interferences from process emissions. Fig. 6 (a) shows the topography of a weld seam section recorded by OCT and 3D macroscopy, respectively. The OCT-based topographic scan contains a very precise representation of the structure of the weld seam surface. A more detailed discussion of the data structure can be found in STADTER ET AL. (2019). Comparing the measurements applied by OCT and macroscopy, a good correlation can be seen. A numerical comparison of the individual pixel distance values can be found in the probability density function in Fig. 6 (b) for aluminum and galvanized steel.

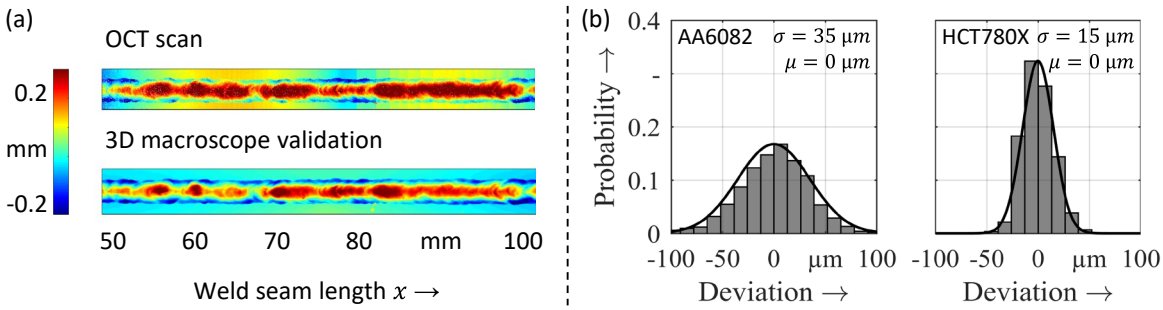

Fig. 6. (a) Topography measured by OCT and macroscope (AA 6082); (b) probability density function of the deviation between OCT and macroscope measurement (line distance 20 µm, point distance 20 µm, scan speed 0.1 m/min; based on STADTER ET AL. (2019))

A standard deviation of 35 µm could be achieved on aluminum and even 15 µm for the measurements on steel. Improvements in the setup of the measurement system will further enhance the accuracy, though the accuracy is already by far sufficient to reliably detect seam characteristics typical for laser beam welding (STADTER ET AL. 2019). The tests on aluminum were also conducted during welding to assess the influence of process emissions. While the offline measurements were carried out at low scanning speeds, the inline measurements were taken at welding speed of 3 m/min. Despite the significantly higher scanning speed and the perturbations from the process, only a marginal drop in measurement accuracy could be noted, from a standard deviation of 35 µm in the offline tests to 41 µm in the inline tests.

7. Conclusions and outlook

A sensor system based on low coherence tomography allowed for topographical measurements in and around the process zone in laser beam welding. Systematic studies were carried out to assess the influence of fundamental parameters and effects on the sensor signal. The accuracy and limits of the system were investigated with a view to a broad range of applications. It could be shown that the OCT system can be used for inline edge tracking, in situ measurements of the capillary depth and recordings of the weld seam topography for quality assurance purposes.

The great potential of the sensor technology can make a significant contribution to laser processes finding large-scale industrial application where limitations still exist today with regard to process control and monitoring options. Further research activities will address approaches of data evaluation to enable a universal and valid interpretation of the sensor data and to facilitate the use of the technology for industrial applications.

Acknowledgements

The results presented were achieved within the RoKtoLas project, which is supported by the German Federal Ministry of Education and Research (BMBF) within the Photonics Research Germany funding program (contract number 13N14555) and supervised by the VDI Technology Center (VDI TZ). We would like to thank the BMBF and the VDI TZ for their support and for the effective and trusting cooperation.

References

Bernardes, Rui; Cunha-Vaz, José (2012): Optical coherence tomography. A clinical and technical update. Heidelberg, New York: Springer (Biological and Medical Physics, Biomedical Engineering).

Blecher, J. J.; Galbraith, C. M.; van Vlack, C.; Palmer, T. A.; Fraser, J. M.; Webster, P. J. L.; DebRoy, T. (2014): Real time monitoring of laser beam welding keyhole depth by laser interferometry. In Science and Technology of Welding and Joining 19 (7), pp. 560–564.

Boer, Johannes F. de; Cense, Barry; Park, B. Hyle; Pierce, Mark C.; Tearney, Guillermo J.; Bouma, Brett E. (2003): Improved signal-to-noise ratio in spectral-domain compared with time-domain optical coherence tomography. In Opt. Lett. 28 (21), p. 2067. DOI: 10.1364/OL.28.002067.

Chinn, S. R.; Swanson, E. A.; Fujimoto, J. G. (1997): Optical coherence tomography using a frequency-tunable optical source. In Opt. Lett. 22 (5), p. 340. DOI: 10.1364/OL.22.000340.

Donges, Axel; Noll, Reinhard (2015): Laser Measurement Technology. Fundamentals and Applications. Heidelberg: Springer (Springer Series in Optical Sciences, 188). Available online at http://dx.doi.org/10.1007/978-3-662-43634-9.

Dorsch, F.; Braun, H.; Pfitzner, D. (2015): Seam tracking for fillet welds with scanner optics. In German Scientific Laser Society (WLT e.V.) (Ed.): Proceedings of the Lasers in Manufacturing Conference (LiM), 22.-25.06.2015, Munich. Munich.

Drexler, W.; Fujimoto, J. G. (2015): Optical coherence tomography. Technology and applications. 2.th ed.: Springer Reference. Available online at http://link.springer.com/book/10.1007/978-3-540-77550-8.

Drexler, Wolfgang (2008): Optical coherence tomography. Technology and applications. Wolfgang Drexler (eds.). Berlin, Heidelberg: Springer (Biological and Medical Physics, Biomedical Engineering).

Fetzer, F.; Boley, M.; Weber, R.; Graf, T. (2017): Comprehensive analysis of the capillary depth in deep penetration laser welding. In S. Kaierle, S. W. Heinemann (Eds.): High-Power Laser Materials Processing: Applications, Diagnostics, and Systems VI. SPIE. San Francisco, California, United States, Saturday 28 January 2017: SPIE (SPIE Proceedings), p. 1009709.

Flournoy, P. A.; McClure, R. W.; Wyntjes, G. (1972): White-light interferometric thickness gauge. In Applied optics 11 (9), pp. 1907–1915. DOI: 10.1364/AO.11.001907.

Fraser, J. M. (2012): Laser process monitoring and automatic control at kHz rates through inline coherent imaging. In C. Phipps (Ed.): International Symposium on High Power Laser Ablation 2012. New Mexico, USA, 30 April–3 May 2012: American Institute of Physics (AIP Conference Proceedings), pp. 492–496.

Huang, D.; Swanson, E.; Lin, C.; Schuman, J.; Stinson, W.; Chang, W. et al. (1991): Optical coherence tomography. In Science 254 (5035), pp. 1178–1181. DOI: 10.1126/science.1957169.

Ji, Y.; Grindal, A. W.; Webster, P. J. L.; Fraser, J. M. (2015): Real-time depth monitoring and control of laser machining through scanning beam delivery system. In J. Phys. D: Appl. Phys. 48 (15), p. 155301.

Kogel-Hollacher, M.; Schoenleber, M.; Bautze, T.; Strebel, M.; Moser, R. (2016): Measurement and Closed-Loop Control of the Penetration Depth in Laser Materials Processing. In : 9th International Conference on Photonic Technologies LANE (2016).

Kogel-Hollacher, M.; Schoenleber, M.; Schulze, J.; Pichot, J. F. (2017): Inline measurement for quality control from macro to micro laser applications. In B. Neuenschwander, C. P. Grigoropoulos, T. Makimura, G. Račiukaitis (Eds.): Laser Applications in Microelectronic and Optoelectronic Manufacturing (LAMOM) XXII. SPIE LASE. San Francisco, California, United States, Saturday 28 January 2017: SPIE (SPIE Proceedings).

Lee, S. K.; Chang, W. S.; Yoo, W. S.; Na, S. J. (2000): A study on a vision sensor based laser welding system for bellows. In Journal of Manufacturing Systems 19 (4), pp. 249–255. DOI: 10.1016/S0278-6125(01)80004-2.

Lee, S. K.; Na, S. J. (2002): A study on automatic seam tracking in pulsed laser edge welding by using a vision sensor without an auxiliary light source. In Journal of Manufacturing Systems 21 (4), pp. 302–315. DOI: 10.1016/S0278-6125(02)80169-8.

Luo, Zhenjun; Dai, Jian S.; Wang, Chenyuan; Wang, Fengli; Tian, Yongli; Zhao, Mingyang (2012): Predictive seam tracking with iteratively learned feedforward compensation for high-precision robotic laser welding. In Journal of Manufacturing Systems 31 (1), pp. 2–7. DOI: 10.1016/j.jmsy.2011.03.005.

Matsui, S.; Goktug, G. (2002): Slit laser sensor guided real-time seam tracking arc welding robot system for non-uniform joint gaps. 2002 IEEE International Conference on Industrial Technology productivity reincarnation through robotics & automation 11-14 December 2002, Shangri-La Hotel, Bangkok, Thailand. Piscataway NJ: IEEE.

Rodríguez-Gonzálvez, P.; Rodríguez-Martín, M.; Ramos, Luís F.; González-Aguilera, D. (2017): 3D reconstruction methods and quality assessment for visual inspection of welds. In Automation in Construction 79, pp. 49–58. DOI: 10.1016/j.autcon.2017.03.002.

Schmoeller, Maximilian; Stadter, Christian; Liebl, Stefan; Zaeh, Michael F. (2019): Inline weld depth measurement for high brilliance laser beam sources using optical coherence tomography. In J. Laser Appl. 31 (2), p. 22409. DOI: 10.2351/1.5096104.

Stadter, Christian; Schmoeller, Maximilian; Zeitler, Martin; Tueretkan, Volkan; Munzert, Ulrich; Zaeh, Michael F. (2019): Process control and quality assurance in remote laser beam welding by optical coherence tomography. In J. Laser Appl. 31 (2), p. 22408. DOI: 10.2351/1.5096103.

Webster, P. J. L.; Wright, L. G.; Ji, Y.; Galbraith, C. M.; Kinross, A. W.; van Vlack, C.; Fraser, J. M. (2014): Automatic laser welding and milling with in situ inline coherent imaging. In Optics letters 39 (21), pp. 6217–6220.